HHS Public Access

Author manuscript

IEEE Trans Biomed Eng. Author manuscript; available in PMC 2017 September 01.

Published in final edited form as:

IEEE Trans Biomed Eng. 2017 September ; 64(9): 1982–1993. doi:10.1109/TBME.2016.2619333.

Glucose Monitoring in Individuals with Diabetes using a Long-Term Implanted Sensor/Telemetry System and Model

Joseph Y. Lucisano, **Timothy L. Routh**, **Joe T. Lin**, and **David A. Gough***

Joseph Y. Lucisano, Timothy L. Routh, and Joe T. Lin are with GlySens Incorporated, 3931 Sorrento Blvd., Suite 110, San Diego, CA 92121. David A. Gough is with the Department of Bioengineering, University of California San Diego, 9500 Gilman Drive, La Jolla, CA 92093-0412, and is a consultant to GlySens and has an equity interest

Abstract

Objective—The use of a fully implanted, first-generation prototype sensor/telemetry system is described for long-term monitoring of subcutaneous tissue glucose in a small cohort of people with diabetes.

Methods—Sensors are based on a membrane containing immobilized glucose oxidase and catalase coupled to oxygen electrodes and a telemetry system, integrated as an implant. The devices remained implanted for up to 180 days, with signals transmitted every 2 minutes to external receivers.

Results—The data include signal recordings from glucose clamps and spontaneous glucose excursions, matched respectively to reference blood glucose and finger-stick values. The sensor signals indicate dynamic tissue glucose, for which there is no independent standard, and a model describing the relationship between blood glucose and the signal is therefore included. The values of all model parameters have been estimated, including the permeability of adjacent tissues to glucose, and equated to conventional mass transfer parameters. As a group, the sensor calibration varied randomly at an average rate of −2.6%/week. Statistical correlation indicated strong association between the sensor signals and reference glucose values.

Conclusions—Continuous, long-term glucose monitoring in individuals with diabetes is feasible with this system.

Significance—All therapies for diabetes are based on glucose control and therefore require glucose monitoring. This fully implanted, long-term sensor/telemetry system may facilitate a new era of management of the disease.

*Correspondence: dgough@ucsd.edu.

Competing interests: J.Y.L., J.T.L., T.L.R. and D.A.G. have equity interests in GlySens, which is the owner and developer of the device and licensee of intellectual property for some aspects of the technology from UCSD. J.Y.L. and D.A.G. are co-founders of GlySens. D.A.G. is a consultant to GlySens, an arrangement approved by the University of California San Diego in accordance with its conflict of interest policies.

Author contributions: sensor design, fabrication and testing was done by J.Y.L., J.T.L. and T.L.R.; modeling, parameter estimation and statistical analysis was done by D.A.G., who had full access to the study data, and takes responsibility for the integrity of the data and accuracy of the analysis. The text was written by J.Y.L. and D.A.G.

Index Terms

long-term glucose monitoring; fully implanted sensor/telemetry system; blood glucose–sensor signal model

I. INTRODUCTION

Glucose control is central to all therapies for diabetes, and achieving control requires monitoring glucose concentration. The landmark Diabetes Control and Complications Trial (or DCCT) [1] and related studies that established the causal relationship between levels of plasma glucose (or “blood glucose”) and the complications of the disease were based on the assay of glycosylated hemoglobin, or HbA1c, which correlates with blood glucose integrated over the previous approximate 90-day period [2] but is not useful for day-to-day glucose management. The DCCT was therefore inherently limited to assessment of control based on averaged blood glucose, but did not include dynamic aspects of control, which may be of equal or greater importance in management of the disease.

The most common method of daily glucose monitoring involves collection of a mixture of capillary blood and tissue fluids by finger prick, or “finger-sticking” [3]. This procedure has the advantage that it can be performed by the individual and provides up-to-the-minute information. However, finger-sticking requires user initiative, is inconvenient or unacceptable to many people with diabetes, and is almost never performed frequently enough to follow actual blood glucose dynamics [4]. Glucose monitoring, if limited to finger-sticking and HbA1c, cannot reliably detect transient hyperglycemic and hypoglycemic blood glucose excursions [5], or support new approaches to the management of diabetes such as the “artificial pancreas” that based on dynamic aspects of glucose control [6].

Continuous daily monitoring of subcutaneous tissue glucose is presently possible with short-term, percutaneous glucose sensors in the form of a needle, or that are flexible and introduced through the skin with needles [7]. The external part of the sensor is connected to a signal processing unit attached to the skin that sends information wirelessly to a monitor and display device. The sensors are based on a reaction between glucose and oxygen catalyzed by immobilized glucose oxidase that produces hydrogen peroxide, which is detected electrochemically. These sensors have certain disadvantages: they must be inserted into the subcutaneous tissues by the user and replaced every 3 to 7 days. The percutaneous access causes unavoidable skin irritation and mechanical micro-motion at the sensor-tissue interface, exacerbating the acute foreign body response and leading to a decay or instability in the signal after insertion requiring finger-sticking typically every 12 hours for sensor recalibration. Further, sensor signals have a variable delay after blood glucose values. Due in part to these limitations, percutaneous sensors to date have served only as adjunctive glucose monitoring devices used in conjunction with finger-sticking, rather than as absolute concentration standards. An ideal continuous glucose sensor would be non-percutaneous, unobtrusive and not attached to the skin, retain stable long-term calibration, and require minimal if any maintenance by the user.

Previous investigators have reported studies of long-term glucose sensors in humans [8]. The sensors were based on the peroxide detection principle, employed a novel porous membrane designed to encourage vascular in growth, and were recalibrated every 1 to 4 weeks. Responses to glucose challenges were fitted by regression with a constant delay, and analyzed qualitatively. There was no attempt to display the range of sensor responses, characterize the tissue permeability or include histologic studies. One sensor functioned for six months, but there were limitations due to tissue hypoxia and increasing delay with time, and implants failed prematurely due to a vigorous inflammatory response, loss of are enzyme activity, water leakage into the telemetry package, and other causes.

We previously reported the development of our sensor system and demonstrated its long-term function in normal and diabetic pigs [9]. Implants were first operated in normal pigs for one year, after which the animals were made diabetic by administration of streptozotocin, and the monitoring continued for an additional five or more months, for as long as 520 days in one case. The experiments included extensive histologic studies and represented a collective total of 31 device-years of implant experience, with 17 implanted devices remaining functional for more than one year.

We have also used this sensor/telemetry system configured without enzymes as a long-term oxygen sensor in pigs to assess the permeability of the subcutaneous tissues adjacent to the implant [10]. These studies involved direct *in situ* measurements of oxygen mass transfer in living tissues surrounding the implant and included the scheduled removal of implants for detailed histologic analysis. The results further demonstrated the feasibility of long-term operation of this type of implanted sensor. There are as yet no such mass transfer measurements for glucose.

We report here results obtained from five individuals with diabetes in a study of this first-generation glucose sensor/telemetry system, three with type 1 diabetes and two with insulin-requiring type 2 diabetes, three of whom were women and two were men. The data consist of 14 recordings from monthly in-clinic glucose excursions (clamp studies) with reference venous blood glucose values, and representative segments of long-term at-home recordings from sensors of spontaneous glucose excursions with comparative finger-stick values. Data suitable for a modeling analysis were taken from implanted sensors during periods of 55, 57, 82, 147 and 181 days, respectively. Clamp studies that did not provide enough stable values to ensure proper sensor calibration are not included here. There were no battery, antenna, or sensor circuitry failures.

The sensor reports dynamic tissue glucose, for which there is no independent reference. A glucose mass transfer model that relates sensor signals to reference blood glucose measurements is therefore included here. Also included are methods for estimation of the model parameters based on the data.

The goal was to determine if long-term glucose monitoring in humans is feasible with this sensor, rather than to conduct a formal clinical trial or obtain reliability statistics representative of commercial-version sensors, which will come later.

The system design is evolving. Clinical trials are currently underway with a smaller second-generation implant employing the same sensing mechanism, but having only 60% of the present device volume [11].

A. The sensing principle

The glucose sensor is based on the following two-step enzymatic reaction catalyzed by glucose oxidase and catalase [9]:

$$\text{glucose} + O_2 + H_2O \rightarrow \text{gluconic acid} + H_2O_2 \quad (1)$$

$$H_2O_2 \rightarrow 1/2\, O_2 + H_2O \quad (2)$$

When catalase is present in excess, the overall reaction is:

$$\text{glucose} + 1/2\, O_2 \rightarrow \text{gluconic acid} \quad (3)$$

The enzymes are crosslinked in a membrane that covers an electrochemical oxygen sensor, which produces a glucose-dependent oxygen flux or current after the enzyme reaction. A second oxygen sensor without enzymes records the background oxygen current, and the difference is the glucose-dependent difference current, which is related to the glucose concentration [9].

B. The implant

The central ceramic disc contains eight 300 μm-diameter platinized platinum working electrodes with associated counter electrodes and Ag/AgCl potential reference electrodes, against which the working electrodes are cathodically polarized for oxygen reduction. The electrodes are covered by a thin electrolyte layer, a protective layer of medical grade polydimethylsiloxane (PDMS), and a secondary membrane of PDMS having wells located over certain of the electrodes for gels containing immobilized glucose oxidase and catalase. The porous polyester pads shown on each side of the implant are for anchoring.

The implant has a hermetically-sealed titanium shell containing a battery and microprocessor-controlled signal conditioning and telemetry circuitry, the shell having a ceramic disc with platinum electrodes on one side and a planar telemetry transmission antenna on the other side. The circuitry includes potentiostats for polarization of the electrodes, logic circuitry for segmentation of the signals, and a telemetry radio similar to that described in detail elsewhere [12]. The transmitter sends signals to an external receiver-decoder every two minutes.

II. METHODS

A. Device Implantation and Removal

Implants were sterilized according to a validated method [13]. Individual sensor/telemetry units were implanted under local anesthesia in abdominal tissue sites in a twenty-five minute outpatient procedure by making a superficial incision 4.5 cm long and dividing the subcutaneous adipose tissue to create a pocket 0.5 to 1.0 cm below the skin surface. The emphasis was on careful separation of the tissue with minimal incision. The implant was placed in the pocket with the sensor surface facing inward and the telemetry transmission antenna facing outward to the skin. The implant was seated in the pocket, the site sutured, and a protective bandage placed on the skin. The sensors were explanted five to six months later with a similar outpatient procedure.

B. Study design

This feasibility study was performed under a United States Food and Drug Administration (USFDA) Investigational Device Exemption (IDE) at the Profil Institute for Clinical Research (Chula Vista, CA) after approval by a human subjects institutional review board (IRB). All participants gave written informed consent. Subjects were blinded to all sensor and clinical lab reference glucose data during the study.

C. Glucose clamps

Glucose clamp studies of 10 to 12 hours duration were performed on each subject one day each month, starting one month after implantation. A Biostator device (Miles Laboratories) was used to control the infusion of glucose and insulin to achieve specified blood glucose levels in the normal, hypoglycemic and hyperglycemic ranges. Venous blood samples were collected through a forearm catheter every ten to fifteen minutes and reference plasma glucose values were determined from the samples using a Yellow Springs Instrument Company (YSI) 2300 STAT Plus glucose analyzer, a widely accepted reference standard.

Between clamp studies, subjects managed their diabetes according to their personal routine established with their health care provider. Subjects were asked to perform at least four finger-stick measurements daily. They were issued recording Accu-Chek finger-stick glucose meters (Roche Diagnostics) for home use, from which data were downloaded at each monthly visit along with the previous month’s sensor data. The meter and the sensor system receiver were synchronized to a master clock and the synchronization verified at each monthly visit.

D. Calibration procedure

Sensors were calibrated retrospectively at each monthly clamp study by adjustment of the sensor calibration coefficient to minimize error when comparing the sensor output to the reference blood glucose samples. The technique included iterative adjustment of a calibration coefficient to minimize the influence of overshoot/undershoot at glucose plateaus, and iteration to obtain a single calibration coefficient to minimize the overall least squares residual error. Following establishment of calibration at each monthly visit, sensor calibration was not otherwise adjusted during the subsequent month of operation.

III. RESULTS

A. Glucose clamps

Monthly glucose clamp challenges were administered in each subject. Data sets shown below are identified by the subject S and clamp C.

Most signals followed blood glucose excursions closely, with certain characteristics. Blood glucose data points were often not distributed randomly around the sensor signals during rising and falling signal segments, but were aligned approximately parallel to sensor signals. The signals either: 1) typically lagged blood glucose changes (seen with rising blood glucose and sometimes with falling blood glucose); 2) occasionally preceded or led blood glucose (seen only with falling blood glucose and then inconsistently, especially in subjects S1, S3, and S5); or, 3) overshot or undershot blood glucose values. A model that relates the tissue sensor signals and reference blood glucose values, and accounts for most of these observations is described below.

There were several long-term outcomes. Certain sensors (e.g., S1) functioned effectively over the entire study period. Other sensors (e.g., S2) initially functioned well, then for unknown reasons, became insufficiently stable for proper calibration, although remaining sensitive to glucose. The reasons for these responses are unknown, but further studies will address these issues. The clamp results presented here are limited to sensors that were readily calibrated.

B. Calibration

Change in the sensitivity of the implanted sensor to blood glucose, or calibration, was determined at each monthly clamp. Recalibration, or the monthly adjustment in sensitivity required to return the signal to the original 100% sensitivity, varied randomly at an average rate of −2.6 %/week for all sensors as a group, consistent with the rate of inactivation of the immobilized enzymes, and is given for individual sensors in Table 1. (The clinical recalibration schedule and method have yet to be established). Results show that the sensitivity to glucose is quasi-linear over the operational range and changes only slightly during use, providing justification for the linear model below.

C. Spontaneous glucose excursions

Examples of spontaneous glucose excursions monitored between clamp studies are shown below. The blue points are discrete 2-minute sensor signals and the red triangles are finger-stick values. Each sensor was calibrated retrospectively after the monthly glucose clamp study, with no further recalibration adjustments throughout the subsequent one-month period. For statistical analysis, sensor values were matched to corresponding finger-stick values and compared without the model.

IV. ANALYSIS

A. The model

Glucose sensors implanted in subcutaneous tissues respond to glucose in the local interstitial fluid, and therefore report interstitial glucose (or “tissue glucose”), rather than blood glucose. The following model describes the dynamic relationship between the blood glucose input and insulin input, when present, and the sensor signals.

The model contains: 1) a glucose diffusion delay in the adjacent tissue, which is a lag due to diffusion from local capillary blood through interstitial spaces to the sensor; 2) a sensor delay, or the response time of the sensor *per se* due to glucose diffusion and reaction within the sensor; 3) an insulin-dependent term for glucose uptake, which accounts for the diffusion-limited consumption of glucose by metabolically active tissues in the vicinity of the sensor when sufficient insulin is present; and 4) noise, or processing error.

In the absence of insulin, the overall transfer function is represented by the diffusion and sensor transfer functions in series. However, when sufficient insulin is present there may exist an additional process of glucose uptake by cells in the vicinity of the sensor, temporarily reducing the local extracellular glucose available to the sensor, and thereby effectively competing with the sensor for access to glucose. During conditions of falling blood glucose, this hypothesized competition may occasionally result in the sensor signal apparently “leading” the blood glucose, an observation that has been reported occasionally with percutaneous sensors [16, 17]. Nevertheless, an overt sensor lead was not routinely observed with every insulin infusion, as a certain minimal local concentration of insulin is apparently required to show the effect. When leads were observed, they were seen only with the higher insulin infusions, and the insulin-dependent lead feature of the model was therefore activated only retrospectively.

The model is based on assumptions that after intravenous infusion, glucose is presented to the vascular bed at the implant site and the sampling catheter simultaneously, and the blood collection and processing time is inconsequential. It was also assumed that endogenous insulin was either absent in these subjects, or insufficient to cause rapid glucose-lowering during clamp studies.

As the sensor signal values were transmitted every two minutes but blood glucose values in clamps were collected only every ten to fifteen minutes, linear interpolation was performed between adjacent blood glucose values to provide reference values for individual pairing with each sensor point. No interpolation was performed in the spontaneous monitoring.

B. Determination of the model structure

The purpose of the model is to describe sensor characteristics and local physiologic processes such as diffusion and glucose uptake that modulate the sensor signal, and estimate their magnitudes and dynamics. A quasi-steady state model structure was sought that depicted the qualitative characteristics of the prototype system, including substrate consumption by the sensor, near-linearity, and simplicity. Previous models proposed for use with percutaneous sensors [e.g., 17, 30, 31] have not included detailed comparisons of

model predictions with sensor signals, estimates of model parameters, or lead features, and in some cases contain reversible terms that are appropriate only for sensors based equilibrium affinity binding processes [e.g., 31]. Such models predict concentration-dependent lags and hysteresis, features that are not found in the present data.

C. Estimation of model parameters

Once the model was identified, model parameters were estimated by positing initial parameter values, inputting blood glucose values into the system, and comparing the predicted results to observed signals. The parameter values were then adjusted iteratively until an acceptable goodness-of-fit between the predicted and observed signal values was obtained. These values were then related to conventional mass transfer parameters to define the glucose permeability of the adjacent tissues. An example of the estimation is shown below.

The model is dimensionless, with the delays scaled to the *in* vitro sensor time constant and the gains scaled to unity sensor calibration. An iterative system identification method [18] implemented in MATLAB was used in conjunction with clamp results to determine the parameter values necessary to achieve an acceptable fit between the discrete blood glucose and signal pairs. The sensor delay τ_s was first determined *in vitro* from the response to a glucose step in well-stirred solutions. The diffusion delay τ_d was next estimated from the signal in the lag region by iteratively approaching the closest fit between the combined sensor and proposed tissue delay value, and the observed sensor signal, with the sensor and tissue gains set at unity. The combined tissue delay τ_z and gain K_t were then estimated from the signal lag-lead region by iteration to achieve parameter values that allowed a goodness-of-fit comparable to that in the lag region. The tissue uptake delay τ_u and gain K_u were calculated from model terms. Model results were validated for the lag region by exchanging the input and output.

D. Summary of parameter estimates

Table 1 below contains a summary of the parameter estimates. The delay terms are scaled to the *in vitro* sensor delay τ_S = 2.42 min (at 0.24 mM oxygen), and the gain terms K_S and K_d are scaled to unity and given in units of %. The “model” column contains goodness-of-fit (gf) values for each clamp in units of %, corresponding to lag and lag-lead regions respectively, or contains a value for the lag region and a “*” symbol where no lead was observed. Entries under the “control” column are goodness-of-fit values for direct comparison of the un-modeled interpolated blood glucose and sensor signals. The “Δ cal”, or change in calibration column, contains values of the monthly adjustment of sensor sensitivity required to return the signal to the original 100% calibration, expressed as % change per week. These values were determined at 150 mg/dl blood glucose concentration, but are similar at other concentrations. The MARD column contains values in units of %, based on lag regions. The R-value, or correlation coefficient [15] describes the strength of association between the interpolated blood glucose reference values and the sensor values for each clamp, with $p < 0.001$ in each case. The mean and standard deviations of column parameter values are given in the last line.

E. Equivalent mass transfer parameter

The estimated lumped parameter values are analogous to conventional distributed mass transfer parameter values obtained by independent physical means. The maximal diffusion delay is equivalent to the conventional time lag expression $L=\delta^2/6D_g$ [19], where δ, the diffusion distance in nearby tissues (225 μm), is estimated from histology studies in animals [9]. This leads to a value of $D_g=2.51\times10^{-7}$ cm^2/s for the implicit effective diffusion coefficient of glucose in tissues, which is consistent with that predicted by semi-infinite body mass transfer solutions [20]. The value is also is comparable to $D_{g,es}=1.89\times10^{-7}$ cm^2/s predicted from Einstein-Stokes scaling by molecular dimensions based on oxygen transport to long-term oxygen sensors in porcine tissues under similar conditions [20]. The reasonable agreement of these values suggests that the permeability of adjacent tissues to small molecules is describable by conventional theory and is sufficient to support function of the implanted sensor over the long term.

The time constant τ_u for the insulin-dependent glucose uptake term is equivalent to the time lag of a glucose diffusion-limited, reaction-diffusion process [21], when sufficient insulin is present locally to allow maximal, glucose-limited uptake. The value of τ_u is therefore expected to be smaller than τ_d, and the gain K_u is expected be smaller than K_d to account for net glucose consumption and negative to coincide with the signal lead. The accuracy of τ_d and K_u is limited by error propagation and the accuracy of the other estimated parameter values used in the calculations, and the values should be considered only approximate.

V. DISCUSSION

A. Indices of accuracy

The Pearson product-moment correlation coefficient R [15], which quantifies the strength of association between the sensor and respective reference values, ranged from 0.84 to 0.98 for individual clamps ($p < 0.001$) and 0.37 to 0.88 for spontaneous excursions. The commonly used consensus error grid [22] and the error grid with constant lag [23], which segregate errors according to the associated corrective clinical actions, gave values of 75.2%, 23.7%, 1.1%, 0%, and 0% in consensus error grid regions A thru E respectively, as determined from the signal plateau regions of the combined glucose clamps. MARD [24], the mean absolute relative difference reported in Table 1 in the lag region ranged from 8.2% to 28.1%, with a median of 16.2% for individual clamps.

Regardless of statistical values, certain features remain unexplained by the model. For example, clamps S1:C2, S1:C3, S1:C4, and S2:C4 show segments in lag regions where sensor values were temporarily lower than reference blood glucose values, but would not have lead to a clinical error. However, certain other clamps, e.g., S1:C6, S2:C2, contain brief segments in which sensor values were higher than normoglycemic values, and potentially problematic. The causes of these discrepancies need further study.

B. Sensor design

This glucose sensor principle based on dual oxygen sensors has several unique advantages for long-term function as an implant. First, glucose oxidase is specific for glucose and the

inner hydrophobic membrane layer between the enzyme and the electrode surface preserves the specificity by preventing otherwise confounding chemical species present in tissue fluid from reacting at the electrode and interfering with the signal. Second, the potentiostatic oxygen sensor design used here has been shown to have exceptional stability and freedom from interference [25, 26]. Third, the enzyme-containing membrane layer incorporates hydrophobic domains that allow access of sufficient oxygen into the enzyme disc to assure that the reaction is limited by glucose, in spite of substantially lower oxygen concentrations in the tissues [26, 27]. Fourth, the sensing principle allows subtraction from the glucose signal of the effects of local physiologic oxygen excursions that affect both electrodes [9, 28], such as: variations in perfusion of the local vasculature due to posture and physical activity, potential changes in permeability of the adjacent tissue, and variations of the local oxygen concentration itself [10]. Fifth, the oxygen detection strategy also permits the inclusion of excess catalase in the membrane to protect glucose oxidase from peroxide-mediated inactivation [29] and prevent tissue irritation due to peroxide release. And, sixth, a large excess of both immobilized enzymes is included to counter the effects of inactivation [29].

C. Oxygen deficit

A key feature of the sensor is the membrane design for ameliorating the oxygen deficit [28], or the concentration difference between the potential extremes of low tissue oxygen (e.g., 5 mmHg or 0.0075 mM) and high blood (400 mg/dl or 22 mM). The oxygen deficit, estimated to be approximately 3,000 in this case, had to be overcome to assure adequate sensitivity to glucose. This disparity was addressed by taking advantage of the reaction stoichiometry (a factor of 2), the higher relative permeability of tissue and sensor membrane material to oxygen over glucose (a factor of approximately 10), and mainly, the differential permeability and dimensions of the enzyme and hydrophobic domains in the sensor membrane (a factor of about 150) [28].

D. Calibration stability

An important feature of this sensor is the relative stability of calibration. This operational characteristic contrasts with that of percutaneous sensors, where the sensor signal decays substantially after insertion due to peroxide-mediated glucose oxidase inactivation, electrochemical interference, and the acute foreign body reaction to the implant, factors that make frequent recalibration of percutaneous sensors by finger-sticking a requirement [7]. In the present sensor, the system is allowed to stabilize for several days after implantation prior to commencement of recording. In addition, the documented stability of the two-enzyme system, unique design of the sensor components, and the demonstrably stable permeability of the adjacent subcutaneous tissues contribute to the overall system stability [9]. The need for only occasional sensor recalibration may be an important clinical advantage.

E. Tissue response

Although there was no attempt to obtain direct histologic documentation of the tissue response to the implant in this study, the observations of calibration stability and sustained tissue permeability provide indirect evidence that whatever foreign body response may have formed had little effect on implant function. In the previous studies in pigs [9, 10] there were

extensive histologic studies of subcutaneous tissues adjacent to the implant [9, 10], and there was no evidence of an impermeable collagenous encapsulation layer often reported elsewhere. There are several possible explanations: 1) the exposed implant materials (PDMS, titanium and crosslinked albumin) are generally considered to be biocompatible; 2) previous tissue culture studies have found no measureable release of irritants, including enzymes, residual sterilants, hydrogen peroxide, or current; 3) the sensor is not tethered to the body surface as are percutaneous sensors, thereby avoiding repeated micro-motion and shear forces at the implant-tissue interface; 4) human (and pig) subcutaneous adipose tissues are more strongly coupled mechanically to underlying tissues than are the more mobile and pliable superficial tissues of mice, rats and dogs used in certain previous studies, and therefore greater mechanical isolation of the implant; and 5) the implantation procedure emphasizes separation of subcutaneous tissues, with very little tissue damage and bleeding. The acceptable tissue response is a key factor in the success of this device.

F. The model

A fundamental feature of the model is that the hypothesized effect of insulin must be included retrospectively when a signal lead is observed during periods of the most rapid rates of glucose fall. Glucose uptake by local tissues presumably requires insulin diffusion from the bloodstream, insulin binding to receptors on cell membranes, and local metabolic consumption of glucose to the point of sufficient local depletion to be observable in the sensor signal. The lead component of the response is needed for a complete description of sensor function, but may be of limited practical advantage in most clinical applications. Users who have recently injected insulin and are experiencing a certain rate of signal decline may activate the lead term in the model processor to temporarily enhance the reported accuracy. This process may be carried out automatically in the artificial pancreas. However, this may be limited only to users in whom the lead effect has been consistently observed. Although observations were limited, the hypothesized lead component seemed to be associated with both type 1 and 2 diabetic subjects. Studies with a larger cohort are needed to address this question.

Of the delays τ_s and τ_d in the model, the dominant delay (i.e., the larger value, slower process) is due to diffusion in the tissue, although the sensor delay is not negligible. This suggests that the main source of signal error was glucose diffusion in the tissues. The rate of glucose diffusion is a consequence of the permeability and vascularization of the tissues adjacent to the implant. When signal leads were present, the rate τ_u and magnitude K_u of insulin-dependent glucose uptake were found to be small relative to the respective tissue lag and gain terms, as expected from physical arguments.

An alternative approach to parameter estimation involves iterative transposition of sensor signals with respect to reference blood glucose values to estimate average signal delays [32]. This approach presumes constant delays and provides limited physical insights.

Some imprecision may have resulted from the use of interpolated blood glucose values for reference in the clamps, segments of missing spontaneous excursion data, and electronic truncation of sensor values. There are also several potential sources of error associated with the model, including: measurement error in the concentration and timing of blood glucose

and individual telemetered values; acceptance of near-perfect goodness-of-fit; and slight nonlinearity. Nevertheless, statistical measures showed strong associations between signal and reference values.

Differences between the 2-minute sampling interval of the sensor and the longer and irregular sampling intervals of the blood and finger-stick reference sampling posed some difficulties. Conventional Nyquist criteria applied to blood glucose dynamics [4] suggests that the maximal interval between regular blood glucose samples needed for reconstruction of rapid glucose excursions is 10 to 12 minutes. Although sensor sampling rate was well within this interval, it was not practical to collect regular blood or finger-stick values within the same interval.

F. Spontaneous glucose excursions

Much of the data in Fig. 3 were found to be nonstationary beyond periods of several days according to conventional criteria [33], which require that the mean, variance, autocorrelation and autocovariance remain invariant to a shift in time. Nonstationarity has been demonstrated previously by direct blood glucose sampling in individuals with and without diabetes [34], indicating that this property is independent of the sensing method. As the sensor and local tissue properties are shown herein to be stationary to a close approximation, the data suggest that the physiologic blood glucose control system (or “plant” [35]) is itself nonstationary. The system may nevertheless still be strict-sense stationary over several-day time scales, and potentially useful to predict near-future signal values [34] and to establish criteria for patient classification based on glucose dynamics [4].

G. Applications of the sensor

The dynamics of the implanted sensor are likely to be rapid compared to the rate-limiting components of the artificial pancreas, including insulin absorption from a subcutaneous infusion site. However, with the anticipated advent of more rapid-acting forms of insulin and high-performance versions of the artificial pancreas, there will be an even greater need for real-time warning.

Regardless of the treatment approach, the unobtrusiveness, stability and longevity of this sensor will lead to automatic adherence with glucose monitoring by the user, in contrast to the present situation where individuals must make frequent decisions about monitoring.

VI. CONCLUSION

Continuous long-term monitoring of tissue glucose with this implanted sensor/telemetry system is feasible. Results show close statistical correlations between the sensor signals and standard reference values. The model accounts for dynamic differences between blood glucose and the sensor signals. The stable, long-term sensitivity to glucose and estimated parameter values indicate that tissue adjacent to the implant can remain permeable to glucose over the long term. The long-term continuous glucose sensor may lead to a new era in the management of diabetes.

Acknowledgments

We thank Paul Clopton for advice on the statistical analysis, and William Jiang, Lorena Alves and Shaghayegh Abbasi for help with the analysis and preparation of the figures.

This work was supported by grants DK64570 and DK77101 (to UCSD) and DK77254 (to GlySens) from the National Institutes of Health. The content is solely the responsibility of the authors and does not necessarily represent the official views of the National Institute of Diabetes and Digestive and Kidney Diseases or the National Institutes of Health.

References

1. The Diabetes Control and Complications Trial Research Group. The effect of intensive treatment of diabetes on the development and progression of long term complications in insulin-dependent diabetes mellitus. N Engl J Med. Sep; 1993 329(14):977–986. [PubMed: 8366922]
2. Koenig RJ, Peterson CM, Jones RL, Saudek C, Lehrman M, Cerami A. Correlation of glucose regulation and hemoglobin AIc in diabetes mellitus. N Engl J Med. Aug; 1976 295(8):417–20. [PubMed: 934240]
3. Olansky L, Kennedy L. Finger-stick glucose monitoring: Issues of accuracy and specificity. Diabetes Care. Apr; 2010 33(4):948–949. [PubMed: 20351231]
4. Rahaghi FN, Gough DA. Blood glucose dynamics. Diabet Tech, Thera. Feb; 2008 10(2):81–94.
5. UK Hypoglycaemia Study Group. Examining Hypoglycaemic risk in diabetes: Effect of Treatment and Type of Diabetes. Diabetologia. Jun; 2007 50(6):1140–1147. [PubMed: 17415551]
6. Advances and Emerging Opportunities in Diabetes Research. A Strategic Planning Report of the Diabetes Mellitus Interagency Coordinating Committee, Chapter 6: Bioengineering Approaches for the Development of an Artificial Pancreas to Improve Management of Glycemia. http://www.niddk.nih.gov/about-niddk/strategic-plans-reports
7. Tamborlane WV, Beck RW, Bode BW, Buckingham B, Chase HP, Clemons R, Fiallo-Scharer R, Fox LA, Gilliam LK, Hirsch IB, Huang ES, Kollman C, Kowalski AJ, Laffel L, Lawrence JM, Lee J, Mauras N, O'Grady M, Ruedy KJ, Tansey M, Tsalikian E, Weinzimer S, Wilson DM, Wolpert H, Wysocki T, Xing D. Juvenile Diabetes Research Foundation Continuous Glucose Monitoring Study Group. Continuous Glucose Monitoring and Intensive Treatment of Type 1 Diabetes. N Engl J Med. Oct; 2008 359(14):1464–1476. [PubMed: 18779236]
8. Gilligan BJ, Shults MC, Rhodes RK, Jacobs PG, Brauker JH, Pintar TJ, Updike SJ. Feasibility of continuous long-term glucose monitoring from a subcutaneous glucose sensor in humans. Diabet Tech, Thera. Feb; 2008 6(3):378–86.
9. Gough DA, Kumosa LS, Lin JT, Routh TL, Lucisano JY. Function of an implanted tissue glucose sensor for more than 1 year in animals. Sci Trans Med. Jul.2010 2(42):42ra53.
10. Kumosa LS, Routh TL, Lin JT, Lucisano JY, Gough DA. Permeability of subcutaneous tissues surrounding long term implants to oxygen. Biomatls. Sep; 2014 35(29):8287–8296.
11. ClinicalTrials.govIdentifier: NCT02345967.
12. McKean BD, Gough DA. A telemetry-instrumentation system for chronically implanted glucose and oxygen sensors. IEEE Trans Biomed Engin. Jul; 1988 35(7):526–32.
13. FDA-accepted consensus standard "ANSI/AAMI/ISO 14160:1998 –Sterilization of (2011). single-use medical devices incorporating materials of animal origin – Validation and routine control of sterilization by liquid chemical sterilants."
14. Boyne MS, Silver DM, Kaplan J, Saudek CD. Timing of Changes in Interstitial and Venous Blood Glucose Measured with a Continuous Subcutaneous Glucose Sensor. Diabetes. Nov; 2003 52(11): 2790–2794. [PubMed: 14578298]
15. Glantz, ST. Primer of Bio-statistics. 7. New York, NY: McGraw Hill Medical; 2012.
16. Sternberg F, Meyerhoff C, Mennel FJ, Mayer H, Bischof F, Pfeiffer EF. Does fall in tissue glucose precede fall in blood glucose? Diabetologia. May; 1996 39(5):609–612. [PubMed: 8739922]
17. Aussedat B, Dupire-Angel M, Gifford R, Klein JAC, Wilson GS, Reach G. Interstitial glucose concentration and glycemia: implications for continuous subcutaneous glucose monitoring. Amer J Physiol, Endocrinol, Metabol. 2000; 278:E716–E728.

18. Ljung, L. System Identification: Theory for the User. 2. Englewood Cliffs, NJ: Prentice-Hall FTR; 1999.
19. Baker DA, Gough DA. Dynamic delay and maximal dynamic error in continuous biosensors. Anal Chem. Apr; 1996 68(8):1292–1297. [PubMed: 8651496]
20. Incropera, FP., DeWitt, DP., Bergman, TL., Lavine, AS. Fundamentals of Heat and Mass Transfer. 6. New York, NY: John Wiley & Sons; 2007.
21. Leypoldt JK, Gough DA. Comments on the penetrant time lag in a diffusion-reaction system. J Phys Chem. 1980; 84(9):1058–1059.
22. Parkes JL, Pardo SLS, Slatin, Ginsberg B. A new consensus error grid to evaluate the clinical significance of inaccuracies in the measurement of blood glucose. Diabetes Care. Jul; 2000 23(7): 143–1148. [PubMed: 10868819]
23. Kovatchev BP, Gonder-Frederick LA, Cox DJ, Clarke WL. Evaluating the accuracy of continuous glucose-monitoring sensors: continuous glucose-error grid analysis illustrated by TheraSense Freestyle Navigator data. Diabetes Care. Aug; 2004 27(8):1922–1928. [PubMed: 15277418]
24. Noujaim SE, Horwitz D, Marhoul J. Accuracy requirements for a hypoglycemia detector: An analytical model to evaluate the effects of bias, precision, and rate of glucose change. J Diabetes Sci Technol. Sep; 2007 1(5):652–668. [PubMed: 19885133]
25. Lucisano JY, Armour JC, Gough DA. In vitro stability of an oxygen sensor. Anal Chem. Mar; 1987 59(5):736–739. [PubMed: 3565773]
26. Armour JC, Lucisano JY, McKean BD, Gough DA. Application of a chronic intravascular blood glucose sensor in dogs. Diabetes. Dec; 1990 39(12):1519–1526. [PubMed: 2245876]
27. Gough DA, Lucisano JY, Tse PHS. A two-dimensional enzyme electrode sensor for glucose. Anal Chem. Jul; 1985 57(13):2351–2357. [PubMed: 4061843]
28. Gough, DA., Jablecki, MC., Lucisano, JY., Catlin, MB. Tissue implantable sensors for measurement of blood solutes. US Patent. 7,248,912. Jul 24. 2007
29. Tse PHS, Gough DA. Time-dependent inactivation of immobilized glucose oxidase and catalase. Biotechnol Bioengin. Apr; 1987 29(6):705–713.
30. Rebrin K, Sheppard FN Jr, Steil GM. Use of subcutaneous interstitial fluid glucose to estimate blood glucose: Revisiting delay and sensor offset. J Diabetes Sci, Technol. Sep; 2010 4(5):1087–1098. [PubMed: 20920428]
31. Schiavon M, Dalla Man C, Dube S, Slama M, Kudva YC, Peyser T, Basu A, Basu R, Cobelli C. Modeling plasma-to-interstitium glucose kinetics from multitracer plasma and microdialysis data. Diabetes Technol, Ther. Nov; 2015 17(11):825–31. [PubMed: 26313215]
32. Kovatchev BP, Shields D, Breton M. Graphical and Numerical Evaluation of Continuous Glucose Sensing Time Lag. Diabetes Technol, Therap. 2009; 11(2):1–5. [PubMed: 19132849]
33. Oppenheim, AV., Schafer, RW. Discrete-Time Signal Processing. Englewood Cliffs, NJ: Prentice Hall; 1989.
34. Bremer T, Gough DA. Is blood glucose predictable from previous values? Diabetes. Mar; 1999 48(3):445–451. [PubMed: 10078542]
35. Chao, PC. Process Control: A First Course with MATLAB. Cambridge, UK: Cambridge University Press; 2000.

APPENDIX

The deterministic part of the model, given in transfer function format [35], is: $\overline{S}=G_S G_t \overline{BG}$, where $\bar{S}$ is the sensor signal, G_S and G_t are the sensor and tissue transfer functions in series, and $\overline{BG}$ is blood glucose. All terms are given in deviation variables in the Laplace domain *s.*

The sensor transfer function is $G_S=\frac{K_S}{(\tau_S S+1)}$, where K_S is the sensor gain and τ_S is the sensor delay G_t, the tissue transfer function, is the sum of two functions in parallel, namely: the glucose diffusion transfer function $G_d=\frac{K_d}{(\tau_d S+1)}$ with gain K_d and diffusion delay τ_d, and the

insulin-dependent glucose uptake transfer function $G_u = \frac{K_u}{(\tau_u S+1)} \cdot \bar{I}$, with the above-threshold dimensionless insulin $\bar{I} = K_I I$, in which the constant K_I and insulin concentration I have appropriate complementary units. K_u is the equivalent uptake gain and τ_u is the effective uptake delay. When the diffusion and uptake transfer functions are combined, the tissue transfer function becomes $G_t = \frac{K_t(\tau_z S+1)}{(\tau_d S+1)(\tau_u S+1)}$, with the gain $K_t = K_d + K_u \bar{I}$, and $\tau_z = \frac{K_d \tau_u + K_u \tau_d}{K_d + K_u}$. K_u is negative to account for the signal lead effect, and $K_d > |K_u|$. A detailed rate expression for the local action of insulin is not given, as the form, rate constants and threshold could not be determined directly from these experiments. When insulin is below threshold or absent, $\bar{I} = 0$ and $G_t = G_d$.

Fig. 1. The glucose sensor/telemetry system implant [9]
The implant is 3.4 cm in diameter and 1.5 cm thick.

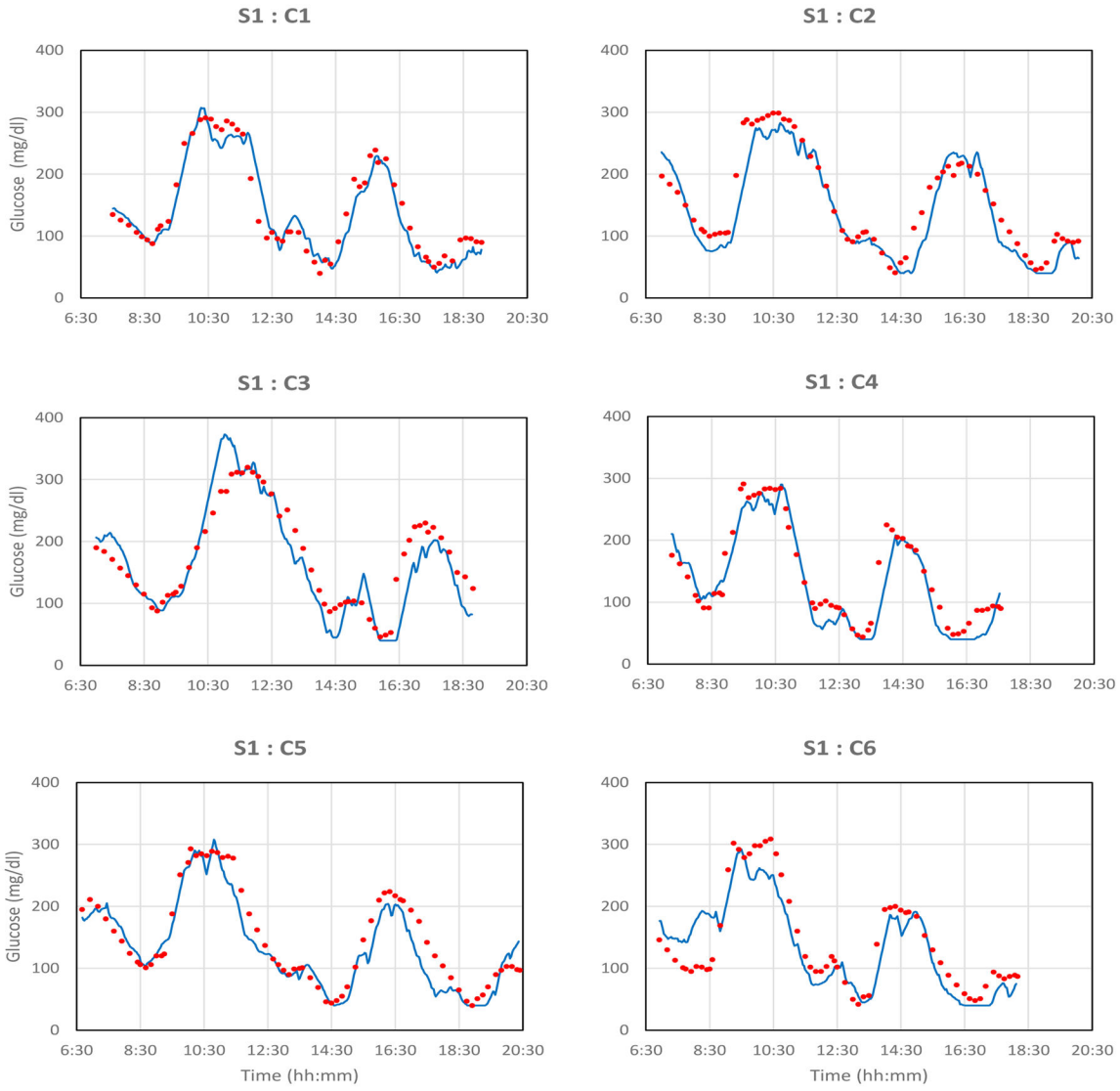

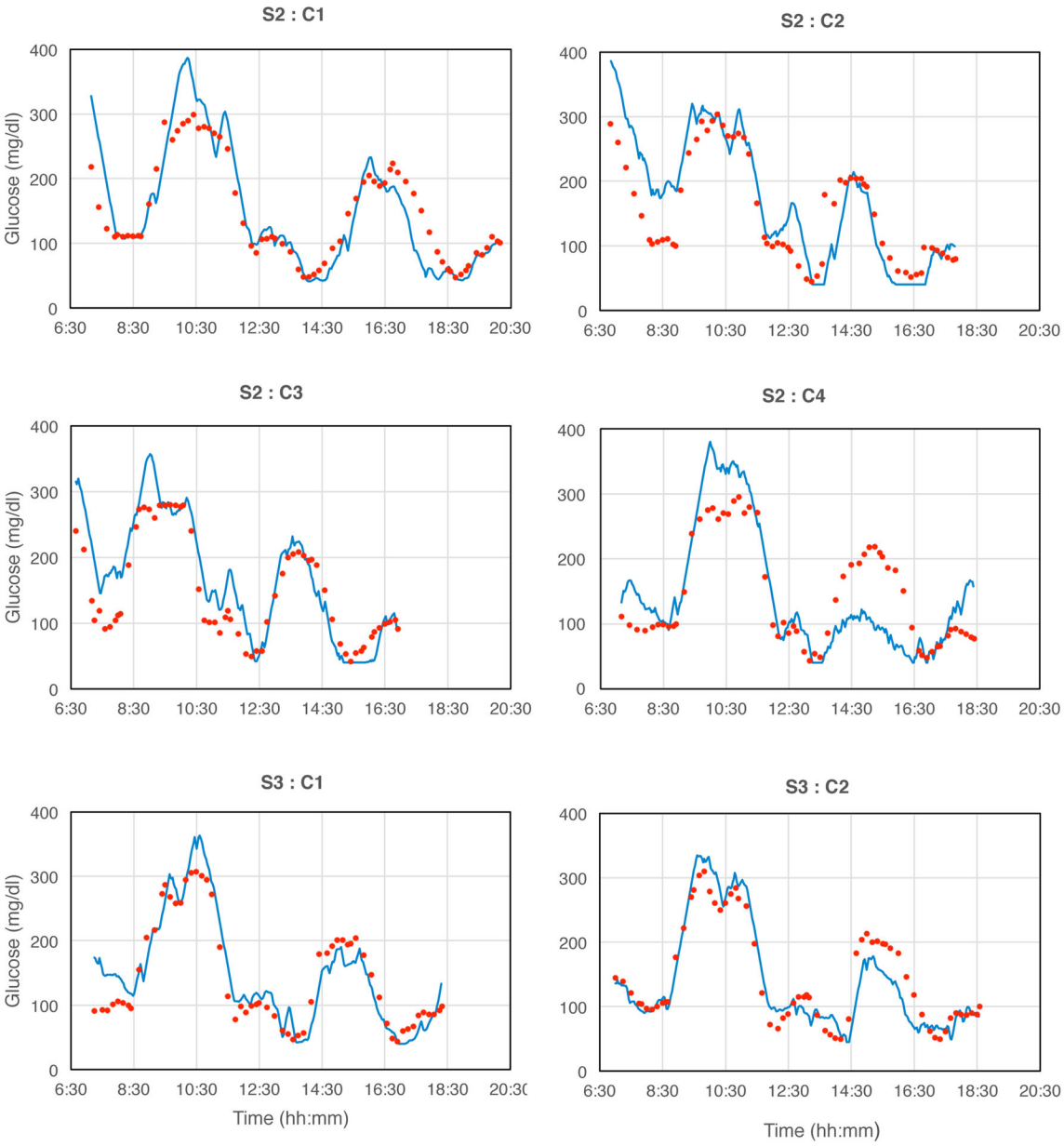

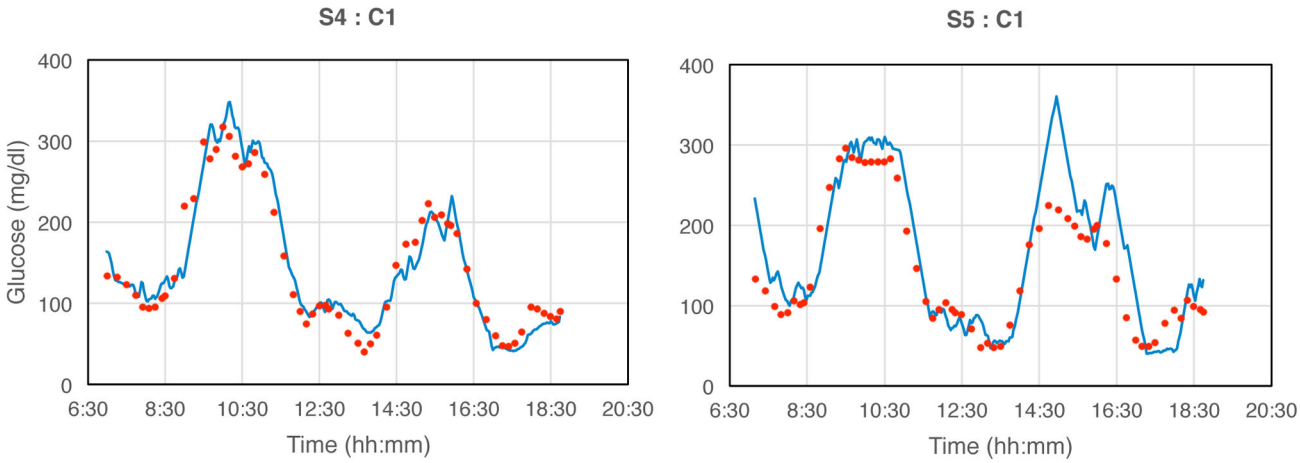

Fig. 2. Monthly glucose excursions created by controlled glucose and insulin infusions

Blue lines: transmitted sensor signals; red points: blood glucose samples from forearm venous catheter assayed with the YSI blood glucose analyzer. The maximal rate of glucose change 3.66 mg/dl·min^{-1}, which is representative of most rapid anticipated excursions in clinical situations [14]. Signals were truncated electronically below 40 and above 400 mg/dl.

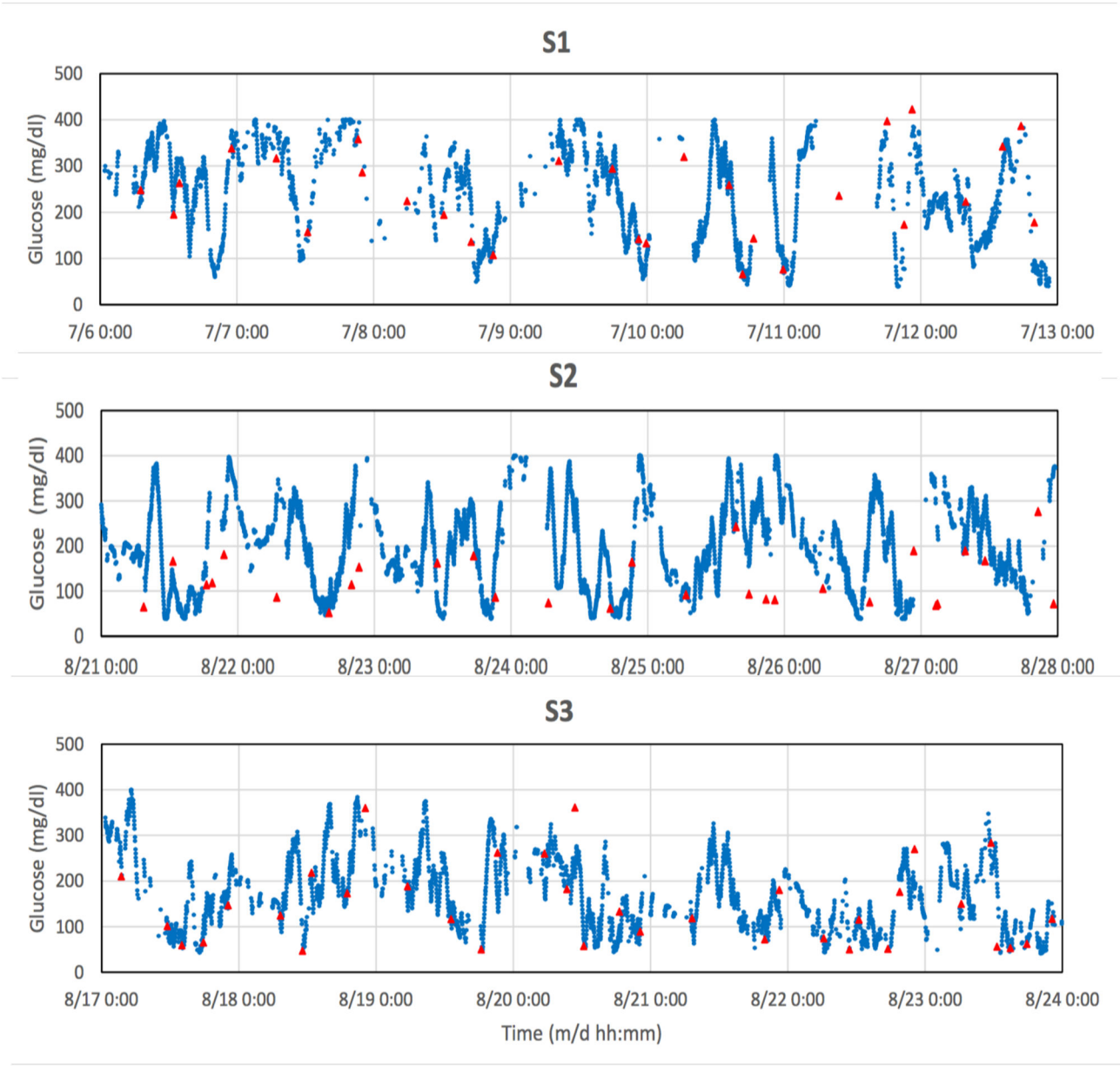

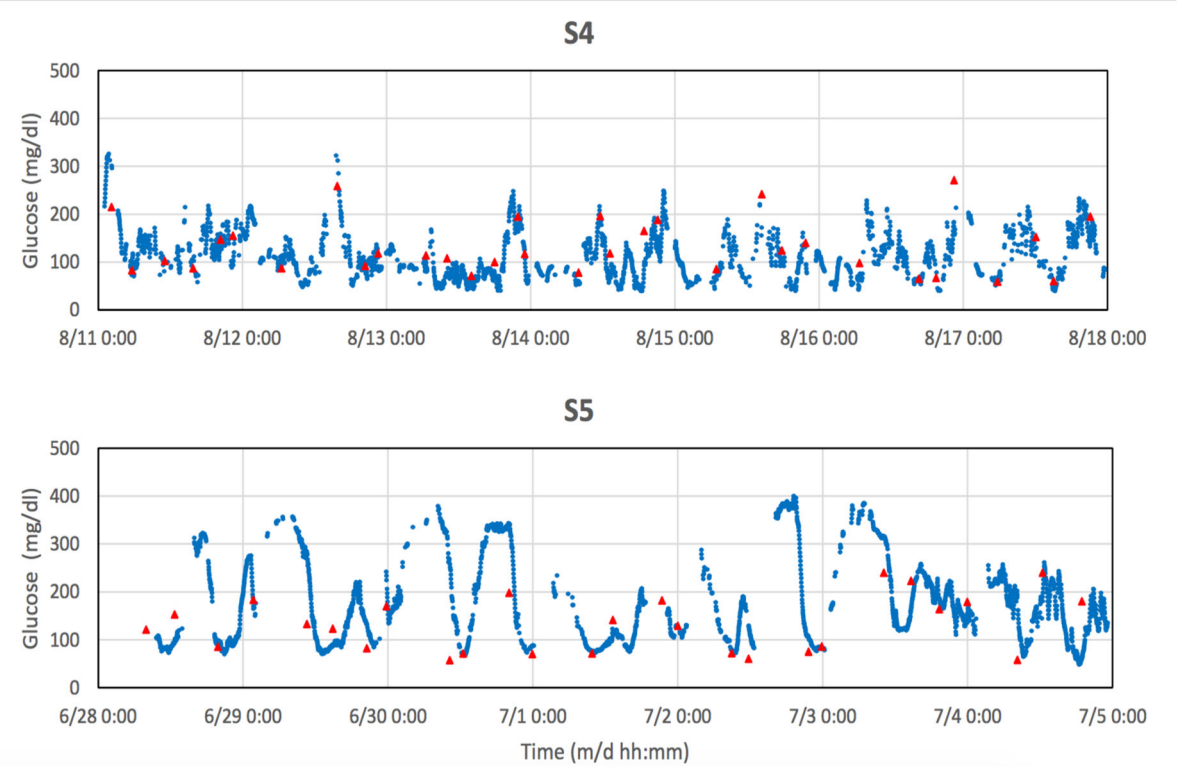

Fig. 3. Examples of monitoring spontaneous glucose excursions

Individual blue data points are 2-min transmitted values; solid red triangles are reference finger-stick glucose values obtained by the subject. Gaps in the sensor data correspond to intervals in which the receiver was temporarily outside of the telemetry range due to user inattention. Signals were truncated electronically below 40 and above 400 mg/dl. Tissue glucose signals were not adjusted to account for lags or leads, and were therefore not expected to exactly match finger-stick glucose values. Statistical correlation R-values [15] were respectively: S1, 0.88; S3, 0.81; S4, 0.80; S5, 0.75; each with $p < 0.001$, and S2, 0.37 ($p < 0.17$).

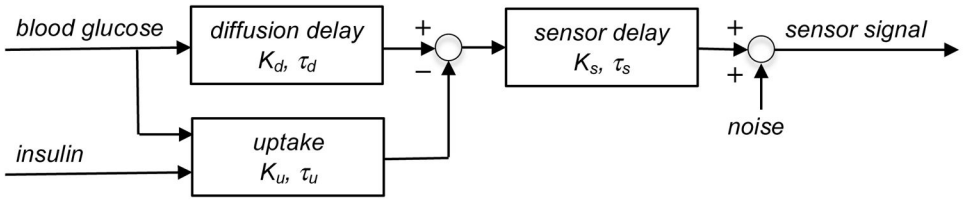

Fig. 4. Model predicting sensor signals from blood glucose and insulin

The glucose diffusion delay and uptake are summed in parallel to give an equivalent tissue delay, which is coupled in series with the sensor delay When insulin is not present or is insufficient, the model contains only sensor and diffusion delays. Noise is due to processing. The mathematical version of the model is given in the Appendix.

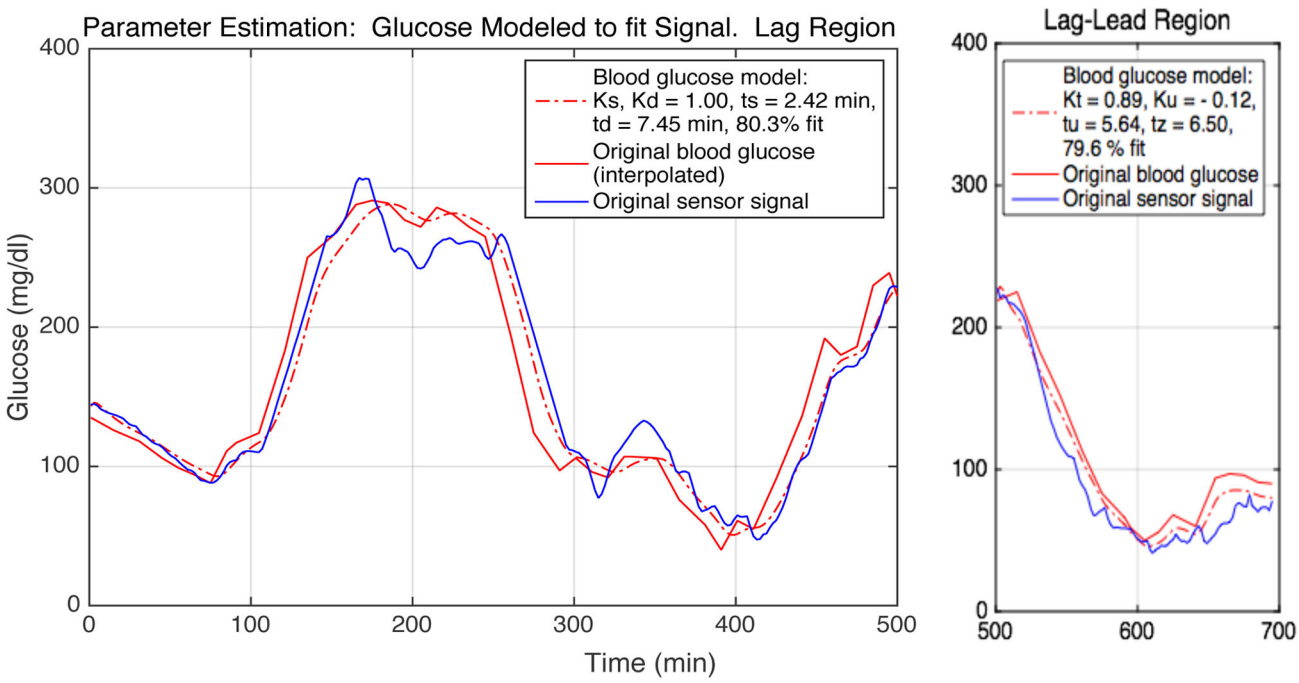

Fig. 5. An example of parameter estimation, S1:C1

The interpolated blood glucose (red, solid line) is modeled (red, broken line) to approximate the original sensor signal (blue), allowing determination of the model parameter values needed to achieve a high goodness-of-fit. The lag and lag-lead regions are separated. Estimated parameter and goodness-of-fit values are given for each data region. The goodness-of-fit, or normalized root mean square error (NRMSE), is

$$\%\text{fit} = 1 - \left\| \frac{y - \hat{y}}{y - \text{mean } y} \right\| \times 100$$

where y is the measured reference value and $\hat{y}$ is the model output value.

Table 1

Summary of estimated parameter values.

subject: clamp	τ_d	τ_u	τ_z	K_u	K_t	model, gf (%)	control, gf (%)	Δ cal, %/wk	MARD, %	R
S1:C1	7.45	5.64	6.50	−0.12	0.89	80.3 79.6	69.3	-	8.2	0.94
S1:C2	10.6	10.5	10.5	−0.30	0.70	84.8 90.1	62.1	+4.3	12.4	0.98
S1:C3	4.79	4.15	4.12	−0.04	0.96	60.9 72.8	56.0	−6.9	10.5	0.88
S1:C4	10.7	8.47	8.25	−0.10	0.90	84.9 83.8	68.1	+0.3	18.0	0.98
S1:C5	7.98	6.67	6.56	−0.08	0.92	77.3 87.0	67.5	−0.3	13.0	0.98
S1:C6	6.92	4.02	2.72	−0.31	0.69	89.6 87.0	51.7	−8.3	24.9	0.93
S2:C1	2.21	0.73	0.62	−0.07	0.93	73.3 88.3	76.2	-	9.1	0.97
S2:C2	2.50	1.67	0.42	−0.60	0.40	67.8 87.6	66.2	−6.2	22.2	0.91
S2:C3	8.82	6.25	2.38	−0.60	0.40	75.5 70.6	66.9	+2.1	23.1	0.92
S2:C4	6.80	*	*	*	1.00	57.2 *	50.3	−5.8	28.1	0.84
S3:C1	2.58	*	*	*	1.00	73.8 *	71.8	-	16.8	0.96
S3:C2	2.51	*	*	*	1.00	78.4 *	76.4	−0.1	12.0	0.96
S4:C1	1.50	*	*	*	1.00	80.8 *	80.7	-	9.7	0.98
S5:C1	2.95	*	*	*	*	75.6 *	73.0	-	19.3	0.94
mean, ± S.D.	5.59, 2.98	5.34, 3.16	4.67, 3.85	−0.25, .223	-	75.7, 83.0 7.81, 5.45	66.9, 9.02	−2.6, 4.1	16.2, 7.04	-

IEEE Trans Biomed Eng. Author manuscript; available in PMC 2017 September 01.